Geochemical Perspectives Letters

Stable strontium isotopes reveal magma-fluid interaction during the evolution of granitic magma

C. Tu[1], X.-Y. Gao[1*], X.-Q. Chen[1], O.G. Safonov[2], M. Ji[1], X.-F. Gu[1], X. Hu[1], Q. Hou[1], F. Huang[1]

https://doi.org/10.7185/geochemlet.2535

Abstract

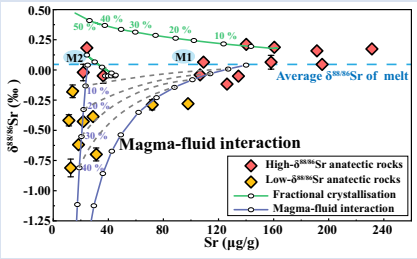

The interaction between granitic magma and fluid at convergent plate margins plays a key role in crustal differentiation and rare metal mineralisation. However, this process remains poorly understood due to the elusive nature of magma and fluid. To address this issue, we reported stable Sr isotope data for anatectic rocks (primarily granitic veins and dikes), melanosomes, and their potential source rocks (mica schist and granitic gneiss) from the Cona area in eastern Himalaya. The anatectic rocks exhibit significantly lower $\delta^{88/86}$Sr than the melanosomes and source rocks. Neither crustal anatexis nor fractional crystallisation significantly contributes to the observed stable Sr isotopic variations. Instead, the variable and extremely low $\delta^{88/86}$Sr values for the anatectic rocks are attributed to the involvement of isotopically light fluids. Geochemical modelling suggests that extremely low $\delta^{88/86}$Sr values of the magmas mostly result from fluid influx into evolving magmas. Thus, stable Sr isotopes emerge as a powerful geochemical tracer of magma-fluid interaction, and are crucial for understanding the petrogenesis of leucogranites and associated rare metal mineralisation in collisional orogens.

Received 12 January 2025 | Accepted 28 July 2025 | Published 16 September 2025

Introduction

Magma-fluid interaction plays a pivotal role in granite evolution, element transport, and rare metal mineralisation (Wu *et al.*, 2020; Zheng and Gao, 2021). Geochemical and petrological studies reveal that granite formation is a result of multiple processes, such as partial melting of source rocks, magma fractional crystallisation, fluid-magma interaction, and wall rock assimilation (Powell, 1984; Cao *et al.*, 2022). However, the complexity and overprinting of geochemical signatures often limit the effectiveness of traditional elemental tracers in uniquely constraining granite genesis (Bartoli, 2021; Cao *et al.*, 2022). In contrast, stable metal isotopes (*e.g.*, Mg, Fe, Zn, K) provide robust tracers for these processes (Teng *et al.*, 2017), making them powerful tools for deciphering multiple processes during granite formation.

Strontium (Sr), which is compatible in feldspar but incompatible in mica, exhibits contrasting partitioning behaviour that makes it particularly useful for investigating melt generation and evolution (Harris *et al.*, 1995). To data, the stable Sr isotopic composition ($\delta^{88/86}$Sr, defined as $[(^{88}Sr/^{86}Sr)_{sample}/(^{88}Sr/^{86}Sr)_{SRM987} - 1] \times 1000$ (‰)) is poorly constrained in terrestrial rocks. The $\delta^{88/86}$Sr values for the Bulk Silicate Earth (BSE) vary from +0.27 to +0.30 ‰ (Moynier *et al.*, 2010; Chen *et al.*, 2022), whereas intermediate to felsic crustal rocks exhibit a broader range from −0.19 to +0.30 ‰ (Ohno *et al.*, 2008; Moynier *et al.*, 2010; Charlier *et al.*, 2012). Such processes as seawater alteration and slab dehydration are thought to preferentially remove isotopically lighter Sr (Amsellem *et al.*, 2018; Klaver *et al.*, 2020; Kani *et al.*, 2023). However, the fractionation coefficients of stable Sr isotopes in crystal-melt-fluid systems remain unknown, as they have not yet been measured in experimental studies or examined from first principles calculations. The mechanisms governing stable Sr isotopic fractionation during metamorphism, partial melting and magma-fluid evolution therefore require further investigation.

In this study, we report high precision stable Sr isotope data for the anatectic rocks (primarily granitic veins and dikes), melanosomes, and their potential source rocks (mica schists and granitic gneisses) from the Cona area, eastern Himalaya, China (Figs. S-1, S-2). In this area, widespread crustal anatexis and migration of felsic melts result in the extensive exposure of migmatites and anatectic rocks including granitic veins, dikes, and leucogranites (Ji *et al.*, 2022, 2023). These anatectic rocks were mainly produced by incongruent partial melting of mica schists and granitic gneisses in the late Oligocene to Miocene (Ji *et al.*, 2021). Detailed geological setting and petrological descriptions of the studied samples are provided in Supplementary Information. The exposure of anatectic rocks, migmatites, and their potential source rocks thus make them well suited for investigating partial melting and granitic magma evolution processes. Our results reveal ~1 ‰ variation in $\delta^{88/86}$Sr values for these anatectic rocks from the Cona area in eastern Himalaya. These findings offer new insights into stable Sr isotope fractionation during partial melting and granite magma evolution and provide a novel approach for understanding the petrogenesis

1. State Key Laboratory of Lithospheric and Environmental Coevolution, School of Earth and Space Sciences, University of Science and Technology of China, Hefei 230026, China
2. Korzhinskii Institute of Experimental Mineralogy, Russian Academy of Sciences, Academician Ossipyan str., 4, Chernogolovka, Moscow district, 142432 Russia
* Corresponding author (email: gaoying@ustc.edu.cn; Tel/Fax : +86-551-63601567)

of Himalayan leucogranites and associated rare metal mineralisation.

Results

The analytical procedures for stable Sr isotopes and the data set are provided in the SI. Uncertainties in the stable Sr isotope measurements are expressed as 2 s.d. (standard deviation), with long term external precision ≤0.03 ‰ for $\delta^{88/86}$Sr values, based on repeated analyses of in-house reference USTC-Sr and GB-Sr. Data quality was monitored by analysing four USGS reference materials (G-2, AGV-2, RGM-1 and BHVO-2), which yielded results consistent with recent literature values (Chen *et al.*, 2022), as shown in Table S-1.

All country rocks, including mica schists and granitic gneisses, show a narrow range of $\delta^{88/86}$Sr values from +0.14 ‰ to +0.40 ‰ (mean = +0.24 ± 0.15 ‰, $n = 8$) (Fig. 1a). The melanosomes have slightly higher $\delta^{88/86}$Sr values from +0.20 ‰ to +0.69 ‰ (mean = +0.36 ± 0.34 ‰, $n = 7$), although their overall variations remain limited (Fig. 1a). In contrast, the anatectic rocks exhibit much lower and more variable $\delta^{88/86}$Sr values, ranging from −0.81 to +0.21 ‰ (mean = −0.15 ± 0.59 ‰, $n = 22$) (Fig. 1a). Based on distinct correlations between $\delta^{88/86}$Sr values and SiO_2 contents, the anatectic rocks are subdivided into two groups (Fig. 1a). These groups also differ in both Sr contents and $\delta^{88/86}$Sr values (Fig. 1b). Group 1 has a wide range in the Sr content (36 to 230 μg/g) but a narrow range in $\delta^{88/86}$Sr values (−0.12 to +0.21 ‰). In contrast, Group 2 shows a relatively narrow range in the Sr content (generally <100 μg/g, typically <30 μg/g) but a broad range in $\delta^{88/86}$Sr values (−0.81 to −0.18 ‰).

Discussion

Stable Sr isotopic fractionation due to chemical weathering and source heterogeneity. The distinct geochemical characteristics of the two groups of anatectic rocks suggest the effects of diverse petrological and geochemical processes. Chemical weathering and source heterogeneity should be considered first to evaluate the origin of stable Sr isotopic variations. The chemical index of alteration (CIA = mol. $Al_2O_3/(Al_2O_3 + CaO + Na_2O + K_2O)$) (Nesbitt and Young, 1982) is an important indicator of the degree

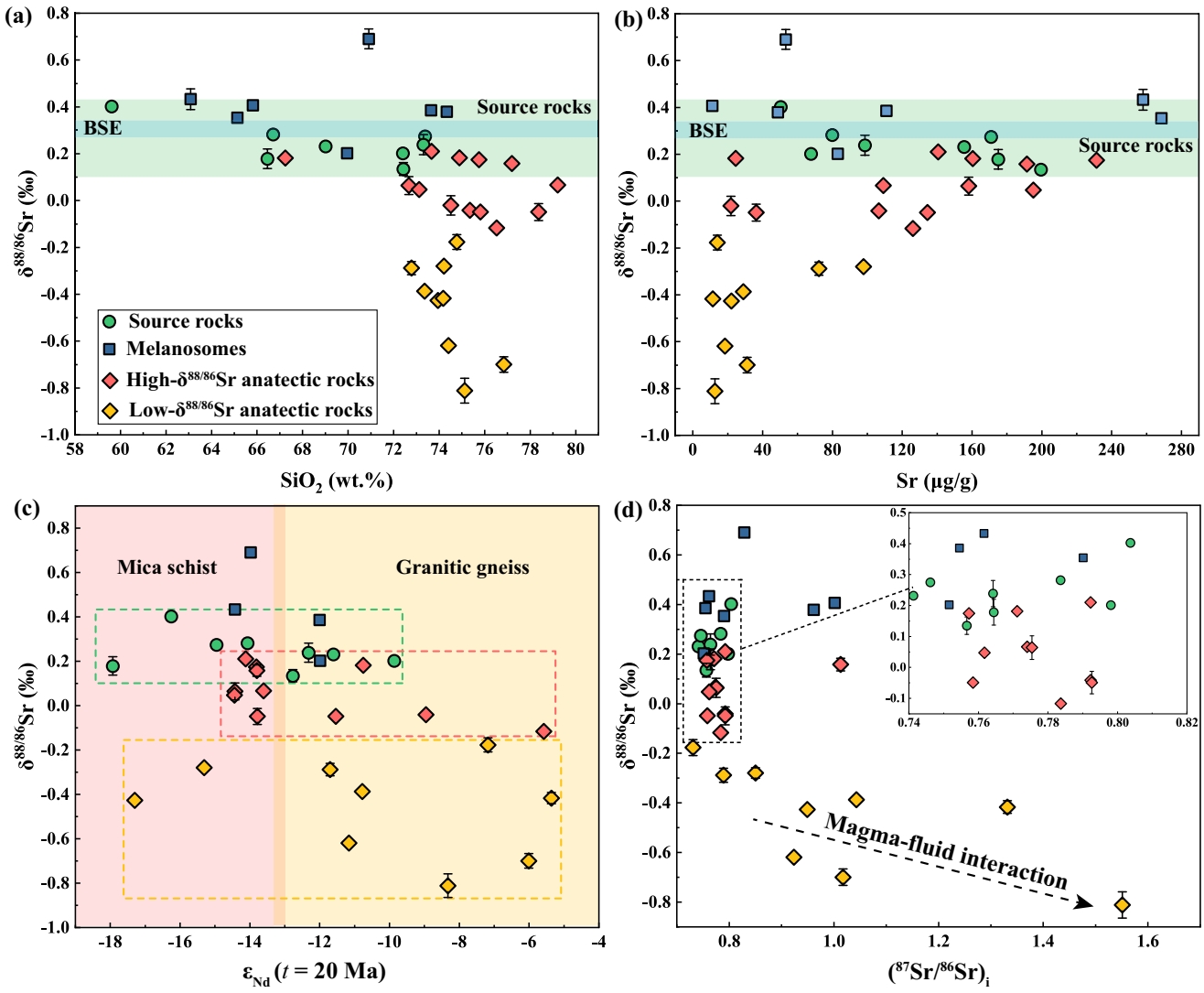

Figure 1 $\delta^{88/86}$Sr *vs.* **(a)** SiO_2, **(b)** Sr, **(c)** $\varepsilon_{Nd}(t)$ and **(d)** $(^{87}Sr/^{86}Sr)_i$. The green and blue shaded regions in **(a)** and **(b)** represent stable Sr isotopic compositions of the source rocks in this study and the BSE as defined by Moynier *et al.* (2010), respectively. The pink and yellow shaded regions in **(c)** represent the $\varepsilon_{Nd}(t)$ ranges of mica schists and granitic gneisses (Ji *et al.*, 2022), respectively. Initial radiogenic Sr and Nd ratios are calculated at $t = 20$ Ma *versus* $^{87}Rb/^{87}Sr$ ratios and $^{147}Sm/^{144}Nd$ ratios.

of chemical weathering. All studied samples have very low CIA values, indicating minimal weathering. The CIA values show no correlation with the $\delta^{88/86}$Sr values (Fig. S-4). In addition, petrological observations confirm that the studied rocks were not strongly overprinted by later alteration. Therefore, the observed $\delta^{88/86}$Sr variations are not attributable to chemical weathering. In the Himalayan orogen, initial Nd isotope compositions calculated at 20 Ma, expressed as $\varepsilon_{Nd}(t)$, effectively distinguish source rock types: mica schists exhibit low $\varepsilon_{Nd}(t)$ values (−19.9 to −13.0), whereas granitic gneisses have higher values (−13.3 to −8.1) (Ji *et al.*, 2022; Zeng *et al.*, 2005). Despite variability in $\varepsilon_{Nd}(t)$ values, both mica schists and granitic gneisses in this study exhibit narrow ranges in of $\delta^{88/86}$Sr values and initial radiogenic Sr isotope compositions calculated at 20 Ma, expressed as $(^{87}Sr/^{86}Sr)_i$ (Fig. 1c,d). Notably, anatectic rocks with both high and low $\delta^{88/86}$Sr values display overlapping $\varepsilon_{Nd}(t)$ values. No correlation between $\delta^{88/86}$Sr and $\varepsilon_{Nd}(t)$ values is observed (Fig. 1c). Thus, source heterogeneity cannot explain the observed variations in $\delta^{88/86}$Sr values. Other processes, such as partial melting of the source rocks, magma fractional crystallisation, and magma-fluid interaction, must therefore be considered.

Stable Sr isotopic fractionation during crustal melting. Anatectic rocks in the Cona area were produced mainly by melting of mica schists and granitic gneisses through the incongruent breakdown of muscovite and biotite (Knesel and Davidson, 2002; Patiño Douce and Harris, 1998), leaving the melanosome residue (Ji *et al.*, 2021). The mineral proportions during this process are dependent on temperature, pressure, and H_2O activity (Patiño Douce and Harris, 1998). Sr contents in melts are mainly controlled by feldspar, which is significantly richer in Sr than mica (Fig. S-5a). We note that higher $(^{87}Sr/^{86}Sr)_i$ values correspond to greater $\delta^{88/86}$Sr values (Fig. 1d). Although different melting reactions of heterogeneous source rock types can account for variable geochemical characteristics, such as $(^{87}Sr/^{86}Sr)_i$ and Sr contents, of the Himalayan leucogranites (Knesel and Davidson, 2002; Gao *et al.*, 2017), the calculated $(^{87}Sr/^{86}Sr)_i$ values do not exceed 0.8, even for melting through the breakdown of biotite (see SI). Therefore, the extremely high $(^{87}Sr/^{86}Sr)_i$ values in the anatectic rocks cannot be attributed to partial melting process.

To investigate the stable Sr isotopic fractionation during partial melting, we conducted phase equilibrium modelling of

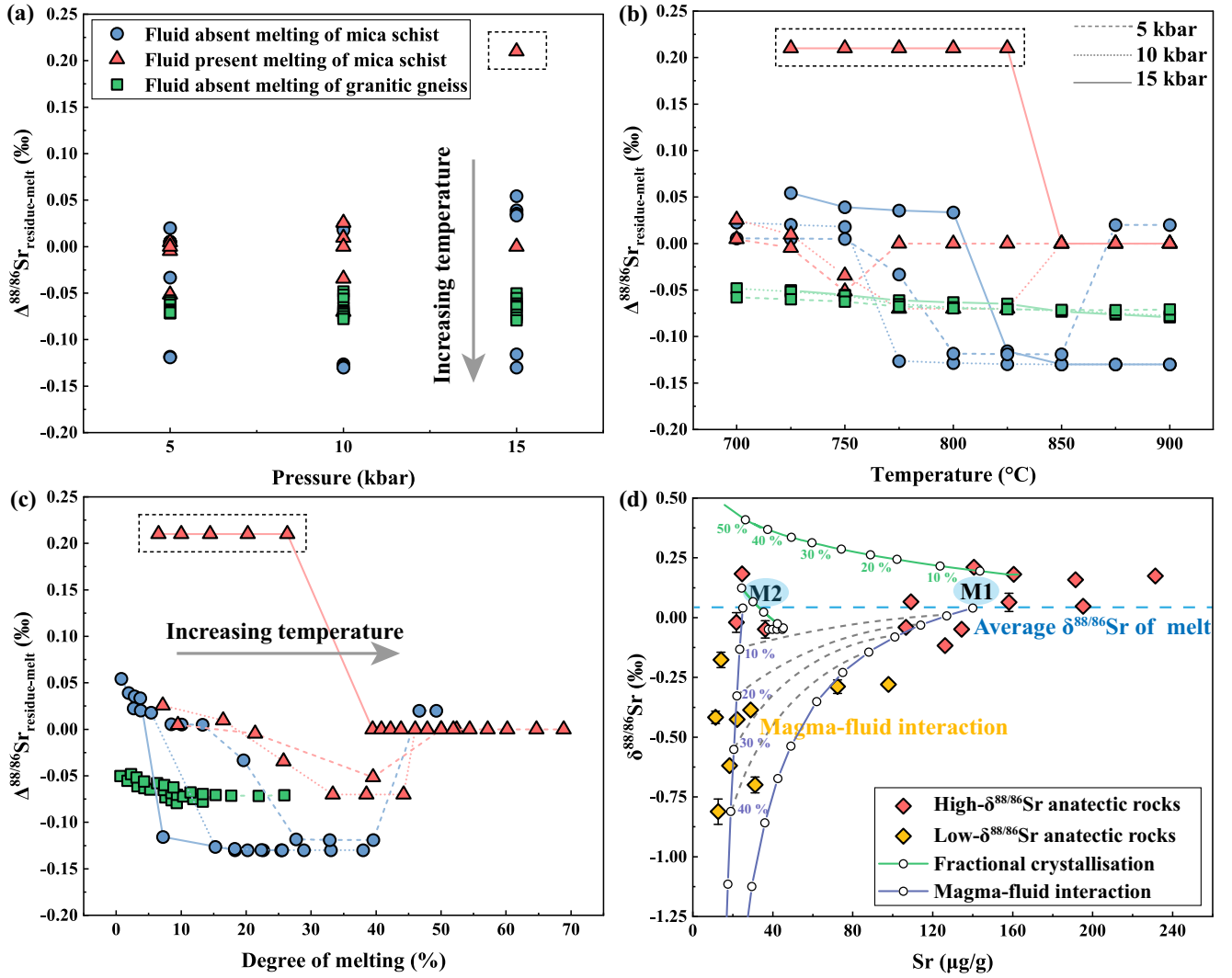

Figure 2 Simulation of partial melting of mica schist and granitic gneiss under different **(a)** pressures, **(b)** temperatures and **(c)** degrees of melting. The dashed box indicates the case of maximum Sr isotopic fractionation. **(d)** Simulation of mixing between melts and fluids. The initial compositions M1 and M2 are set as melt end members in the model. The dashed grey lines are the contours of the amount of fluids. Numbers on the lines denote the fraction of feldspar separation (green line) and the fraction of fluid (purple lines), respectively.

mica schist and granitic gneiss using the Perple_X software combined with geochemical modelling based on mass balance equation (see SI). The mineral assemblages and model proportions of minerals and melt under different anatectic conditions were directly obtained from the phase equilibrium modelling, whereas the Sr contents in the melt and residue were calculated according to batch melting equations (see Table S-4). The average $\delta^{88/86}$Sr value of mica schists ($\delta^{88/86}Sr = +0.29$ ‰) and granitic gneiss ($\delta^{88/86}Sr = +0.22$ ‰) were selected as the primary values, and the estimated fractionation between minerals and melt ($\Delta^{88/86}Sr_{Pl\text{-}melt} = +0.02$ ‰; $\Delta^{88/86}Sr_{Kfs\text{-}melt} = -0.13$ ‰; $\Delta^{88/86}Sr_{Ms\text{-}melt} = +0.21$ ‰; $\Delta^{88/86}Sr_{Bt\text{-}melt} = -0.07$ ‰) based on the observations in this study were used (see SI). The modelled results indicate that partial melting would produce limited Sr isotopic fractionation ($\Delta^{88/86}Sr_{residue\text{-}melt} < +0.10$ ‰ in most cases) (Fig. 2a,b,c). This agrees with observations that the $\delta^{88/86}$Sr values for most melanosomes and some leucosomes overlap with the values for their source rocks. Only fluid-present melting of mica schist under high pressure and low temperature yields larger fractionation ($\Delta^{88/86}Sr_{residue\text{-}melt} = +0.21$ ‰), which is able to explain the heaviest $\delta^{88/86}$Sr value of 0.69 ‰ for one melanosome (Figs. 1b, 2a,b,c). Therefore, partial melting cannot account for the extremely low $\delta^{88/86}$Sr values for the studied anatectic rocks.

Stable Sr isotopic fractionation during fractional crystallisation. Fractional crystallisation has a significant impact on geochemical characteristics of the Himalayan leucogranites (Wu *et al.*, 2020; Cao *et al.*, 2022). Since Eu is strongly compatible in plagioclase and Ba is more compatible than Rb in feldspar, the Ba/Rb ratio and europium anomaly (Eu/Eu*) are useful indicators of fractional differentiation. In high-$\delta^{88/86}$Sr anatectic rocks, Ba/Rb ratios decrease while $\delta^{88/86}$Sr values remain relatively constant. In contrast, low-$\delta^{88/86}$Sr anatectic rocks exhibit significant stable Sr isotopic variations with little change in Ba/Rb ratios (Fig. 3a). Although Sr removal *via* feldspar separation is supported by the correlation between Sr contents and Eu/Eu*ratios (Fig. S-6d), $\delta^{88/86}$Sr values show no correlation with

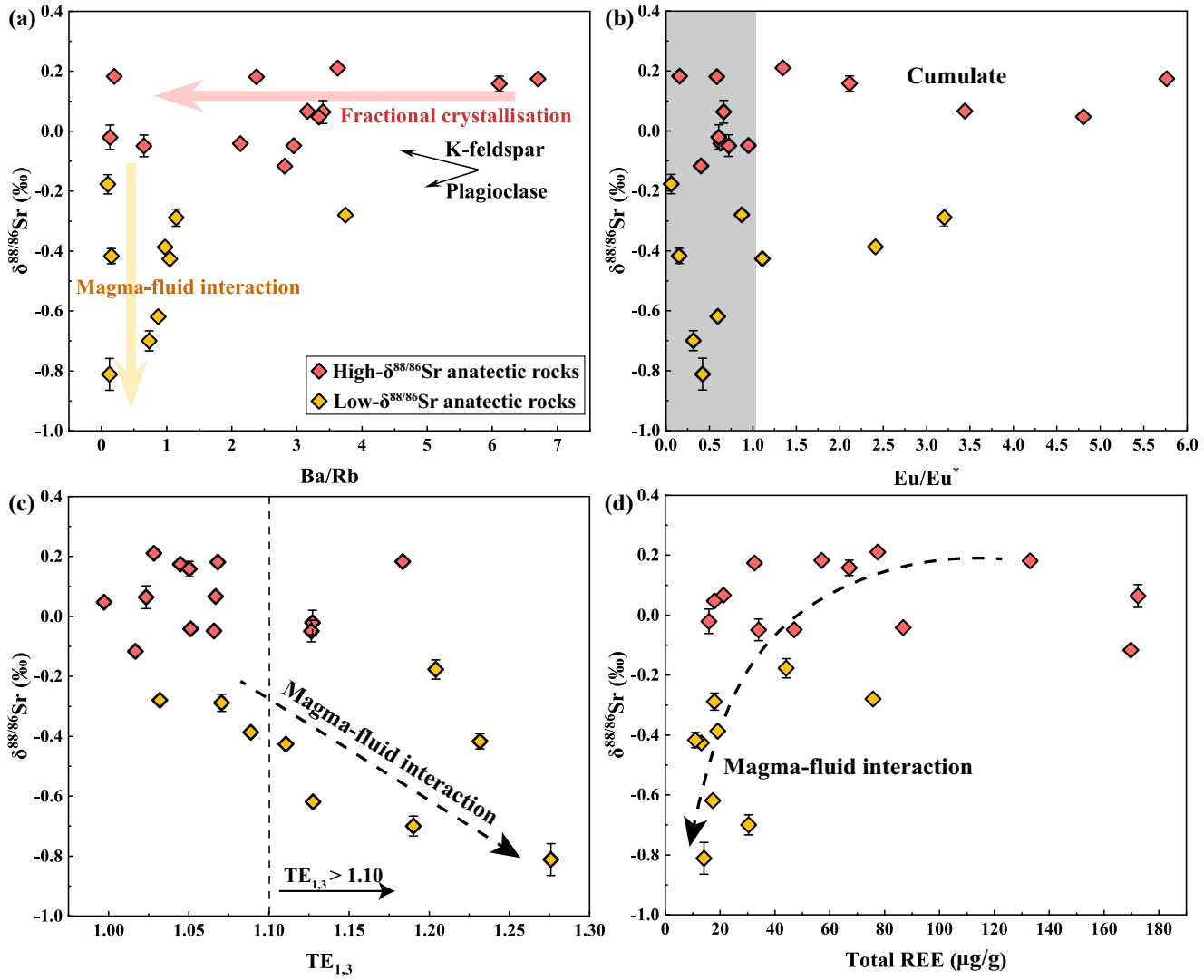

Figure 3 $\delta^{88/86}$Sr *vs.* **(a)** Ba/Rb, **(b)** Eu/Eu*, **(c)** $TE_{1,3}$ and **(d)** Total REE. **(a)** The red and yellow arrows indicate the direction of fractional crystallisation and magma-fluid interaction, respectively. The different effects caused by plagioclase and K-feldspar are indicated by two black arrows. **(b)** Grey shading area covered anatectic rocks with Eu/Eu* < 1 representing differentiated melt. The Eu anomaly is calculated by the equation: $Eu/Eu^* = Eu_N/\sqrt{Sm_N \times Gd_N}$. **(c)** $TE_{1,3}$ is calculated by the following equation (Irber, 1999): $TE_{1,3} = (t1 \times t3)^{0.5}$, where $t1 = [Ce_N/(La_N^{2/3} \times Nd_N^{1/3}) \times Pr_N/(La_N^{1/3} \times Nd_N^{2/3})]^{0.5}$; $t3 = [Tb_N/(Gd_N^{2/3} \times Ho_N^{1/3}) \times Dy_N/(Gd_N^{1/3} \times Ho_N^{2/3})]^{0.5}$. The subscript "N" denotes normalisation to chondritic values (Sun and McDonough, 1989). Black arrows indicate changes of stable Sr isotopes with $TE_{1,3}$ and total REE contents in **(c)** and **(d)**.

Eu/Eu* in samples with Eu/Eu* < 1 (Fig. 3b). This indicates that the $\delta^{88/86}Sr$ variations are not controlled by fractional crystallisation.

Anatectic rocks with Eu/Eu* > 1, representing cumulates, generally exhibit overlapping $\delta^{88/86}Sr$ values (Fig. 3b). To investigate stable Sr isotope fractionation during fractional crystallisation, we performed phase equilibrium modelling using the Perple_X software (see SI). Note that Sr contents in the primary melts would have a large range during partial melting of mica schist and granitic gneiss (Table S-4). Two representative anatectic rocks with different Sr contents (C_{Sr} = 161 μg/g and $\delta^{88/86}Sr$ = +0.18 ‰; C_{Sr} = 36 μg/g and $\delta^{88/86}Sr$ = −0.05 ‰) were selected in the modelling as representative compositions of the primary melts. The mineral assemblage and model proportion of minerals and melt under different crystallisation conditions were directly estimated from the phase equilibrium modelling (Table S-5). The same fractionation factors between minerals and melt as in the partial melting modelling were used. Rayleigh fractionation models were depicted in the Figure 2d. The modelling results show that fractional crystallisation would not produce large variations in $\delta^{88/86}Sr$ values for the differentiated melts, consistent with high-$\delta^{88/86}Sr$ anatectic rocks (Fig. 2d). Thus, the extremely low $\delta^{88/86}Sr$ values for anatectic rocks cannot be explained by fractional crystallisation.

Stable Sr isotopic fractionation during magma-fluid interaction. The most plausible process responsible for the extremely low $\delta^{88/86}Sr$ and high $(^{87}Sr/^{86}Sr)_i$ values for the Sr-poor anatectic rocks is the interaction of their magma with high temperature fluids. Metasomatic textures and fluid inclusions in quartz provide direct evidence for such interactions (Fig. S-3). Rare earth elements (REE) form complexes with non-bridging oxygen, F^-, and Cl^- in fluids, generating tetrad effects (expressed as $TE_{1,3}$) and reducing REE content during magma-fluid interaction (Bau, 1996; Irber, 1999). The correlations between $\delta^{88/86}Sr$ values and these sensitive proxies further support the influence of magma-fluid interaction on stable Sr isotope compositions (Fig. 3c,d). In addition, the elevated $(^{87}Sr/^{86}Sr)_i$ values for the anatectic rocks cannot be explained by partial melting or fractional crystallisation processes, indicating infiltration of external fluids (Fig. 1d). Fluids are known to preferentially carry light Ba isotopes ($\delta^{138/134}Ba$) (Guo *et al.*, 2020). Since Ba and Sr share similar geochemical properties, light Sr isotopes are similarly favoured by fluids (Amsellem *et al.*, 2018, Klaver *et al.*, 2020; Kani *et al.*, 2023). Therefore, fluid influx is inferred to introduce light stable Sr isotopes.

According to the above discussion, it is clear that external fluids with low $\delta^{88/86}Sr$ are required to explain light Sr isotope compositions in the anatectic rocks. To quantify this effect, a simplified two end member mixing model was applied (SI). The Sr contents in Himalayan granites are generally less than 100 μg/g (Cao *et al.*, 2022). Since partitioning coefficient of Sr between fluid and melt ($D_{Sr}^{fluid/melt}$ < 0.3) is low (Borchert *et al.*, 2010), a fluid exsolved from a magma reservoir is predicted to be extremely poor in Sr (<30 μg/g). Alternatively, the external fluids can also be supplied *via* metamorphic dehydration dominated by decomposition of mica, whose Sr content is low. In this regard, we reasonably set the Sr content in the fluids to be 10 μg/g. In addition, since the high-$\delta^{88/86}Sr$ anatectic rocks represent products of partial melting and fractional crystallisation, two initial points with the average $\delta^{88/86}Sr$ value and different Sr contents were selected as the end members in modelling (M1: C_{Sr} = 140 μg/g, $\delta^{88/86}Sr$ = +0.04 ‰; M2: C_{Sr} = 25 μg/g; $\delta^{88/86}Sr$ = +0.04 ‰). If 20–40 % fluids, which is carrying capacity in granitic magma (Thomas and Davidson, 2016; Deng *et al.*, 2024), was adopted in the modelling, then the modelling results in the $\delta^{88/86}Sr$ value of −4.0 ‰ in fluids. Such an extremely light isotopic composition in fluids was also determined for Ba isotope system (Deng *et al.*, 2024). It is worth mentioning that using higher Sr contents in the modelling will make slightly heavier Sr isotope in fluids. In a nutshell, stable Sr isotopic compositions

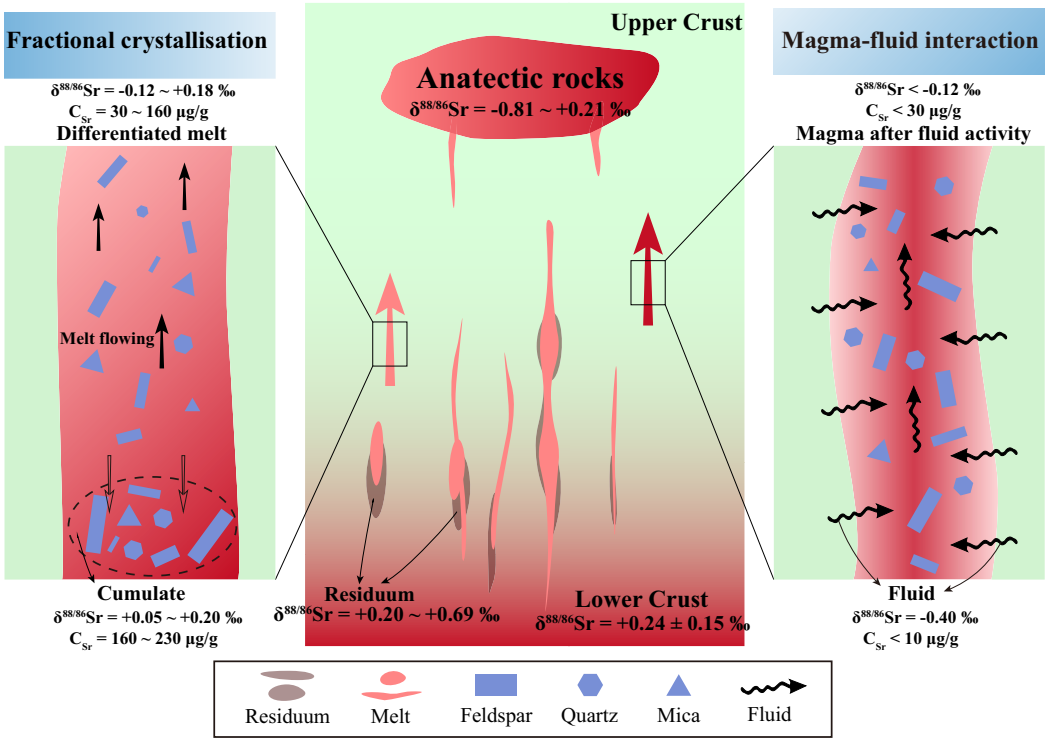

Figure 4 Schematic diagram depicting our current understanding of stable Sr isotopic behaviour during formation and evolution of felsic melts. See text for details.

for the anatectic rocks with low Sr content are more susceptible to be reduced by interaction between melts and fluids (Fig. 2d).

Implications for stable Sr isotopic variation in high silica granites and magmatic evolution. Understanding the differentiation processes of felsic magmas is crucial for elucidating the origin of granites and related rare metal mineralisation. Highly fractionated leucogranites of the Himalayan orogen are enriched in Be-, Nb-, Ta-, and Li-bearing minerals showing significant ore forming potential (Wu *et al.*, 2020). The formation of these leucogranites involved partial melting of source rocks, magma fractional crystallisation, and magma-fluid interaction. Notably, rare metal mineralisation is often closely associated with pegmatites that formed during late stage magmatic evolution with voluminous participation of fluids (Wu *et al.*, 2020). Thus, recognising and tracing fluid activity is essential for understanding both magmatic evolution and associated ore mineralisation. However, quantifying the extent of fluid activity remains challenging. While tetrad REE patterns are widely considered qualitative indicators of magma-fluid interaction, they provide limited constraints on fluid volume or other quantitative information (Irber, 1999). Our study is the first to reveal substantial stable Sr isotopic variations between anatectic rocks (Fig. 4). Importantly, neither partial melting nor fractional crystallisation produces significant variation in stable Sr isotopes, despite their effects on Sr contents in melts. Only melt-fluid interaction could induce substantial stable Sr isotopic variations (Fig. 4).

Thus, stable Sr isotopes emerge as a novel geochemical tracer for identifying fluid activity in the granitic magma systems. Furthermore, systematic correlations among Sr, Ba, and Rb contents and their corresponding stable isotopes may provide a powerful framework for constraining the evolution of felsic magmas (Hu *et al.*, 2022; Deng *et al.*, 2024).

Acknowledgements

This study was supported by funds from the National Key R and D programme of China (2024YFF0807302), the National Science Foundation of China (42472076 and 42330806), the Fundamental Research Funds for the Central Universities, and joint Russian Scientific Foundation – National Science Foundation of China (RSCF-NSFC) project (W2412052 and 25-47-00073). We are grateful to two anonymous reviewers for their thorough and constructive comments that greatly improved the paper. We also express our appreciation to Editor Raul O. C. Fonseca for his editorial handling.

Editor: Raul O.C. Fonseca

Additional Information

Supplementary Information accompanies this letter at https://www.geochemicalperspectivesletters.org/article2535.

Cite this letter as: Tu, C., Gao, X.-Y., Chen, X.-Q., Safonov, O.G., Ji, M., Gu, X.-F., Hu, X., Hou, Q., Huang, F. (2025) Stable strontium isotopes reveal magma-fluid interaction during the evolution of granitic magma. *Geochem. Persp. Let.* 36, 54–60. https://doi.org/10.7185/geochemlet.2535

References

Amsellem, E., Moynier, F., Day, J.M.D., Moreira, M., Puchtel, I.S., Teng, F.-Z. (2018) The stable strontium isotopic composition of ocean island basalts, mid-ocean ridge basalts, and komatiites. *Chemical Geology* 483, 595–602. https://doi.org/10.1016/j.chemgeo.2018.03.030

Bartoli, O. (2021) Granite geochemistry is not diagnostic of the role of water in the source. *Earth and Planetary Science Letters* 564, 116927. https://doi.org/10.1016/j.epsl.2021.116927

Bau, M. (1996) Controls on the fractionation of isovalent trace elements in magmatic and aqueous systems: evidence from Y/Ho, Zr/Hf, and lanthanide tetrad effect. *Contributions to Mineralogy and Petrology* 123, 323–333. https://doi.org/10.1007/s004100050159

Borchert, M., Wilke, M., Schmidt, C., Rickers, K. (2010) Rb and Sr partitioning between haplogranitic melts and aqueous solutions. *Geochimica et Cosmochimica Acta* 74, 1057–1076. https://doi.org/10.1016/j.gca.2009.10.033

Cao, H.-W., Pei, Q.-M., Santosh, M., Li, G.-M., Zhang, L.-K., Zhang, X.-F., Zhang, Y.-H., Zou, H., Zai, Z.-W., Lin, B., Tang, L., Yu, X. (2022) Himalayan leucogranites: A review of geochemical and isotopic characteristics, timing of formation, genesis, and rare metal mineralization. *Earth-Science Reviews* 234, 104229. https://doi.org/10.1016/j.earscirev.2022.104229

Charlier, B.L.A., Nowell, G.M., Parkinson, I.J., Kelley, S.P., Pearson, D.G., Burton, K.W. (2012) High temperature strontium stable isotope behaviour in the early solar system and planetary bodies. *Earth and Planetary Science Letters* 329–330, 31–40. https://doi.org/10.1016/j.epsl.2012.02.008

Chen, X.-Q., Zeng, Z., Yu, H.-M., Sun, N., Huang, F. (2022) Precise measurements of $\delta^{88/86}$Sr for twenty geological reference materials by double-spike MC-ICP-MS. *International Journal of Mass Spectrometry* 479, 116883. https://doi.org/10.1016/j.ijms.2022.116883

Deng, G., Jiang, D., Li, G., Xu, Z., Huang, F. (2024) Barium isotope evidence for a magmatic fluid-dominated petrogenesis of LCT-type pegmatites. *Geochemical Perspectives Letters* 31, 14–20. https://doi.org/10.7185/geochemlet.2426

Gao, L.-E., Zeng, L., Asimow, P.D. (2017) Contrasting geochemical signatures of fluid-absent versus fluid-fluxed melting of muscovite in metasedimentary sources: The Himalayan leucogranites. *Geology* 45, 39–42. https://doi.org/10.1130/G38336.1

Guo, H., Li, W.-Y., Nan, X., Huang, F. (2020) Experimental evidence for light Ba isotopes favouring aqueous fluids over silicate melts. *Geochemical Perspectives Letters* 16, 6–11. http://dx.doi.org/10.7185/geochemlet.2036

Harris, N., Ayres, M., Massey, J. (1995) Geochemistry of granitic melts produced during the incongruent melting of muscovite: Implications for the extraction of Himalayan leucogranite magmas. *Journal of Geophysical Research: Solid Earth* 100, 15767–15777. https://doi.org/10.1029/94JB02623

Hu, X., Nan, X., Liu, X., Huang, F. (2022) Rubidium isotope compositions of the average upper continental crust and the Himalayan leucogranites: Implications for magmatic-fluid interaction. *Geochimica et Cosmochimica Acta* 336, 165–176. https://doi.org/10.1016/j.gca.2022.09.015

Irber, W. (1999) The lanthanide tetrad effect and its correlation with K/Rb, Eu/Eu*, Sr/Eu, Y/Ho, and Zr/Hf of evolving peraluminous granite suites. *Geochimica et Cosmochimica Acta* 63, 489–508. https://doi.org/10.1016/S0016-7037(99)00027-7

Ji, M., Gao, X.-Y., Zheng, Y.-F., Meng, Z.-Y., Gao, P. (2021) Metapelites record two episodes of decompressional metamorphism in the Himalayan orogen. *Lithos* 394–395, 106183. https://doi.org/10.1016/j.lithos.2021.106183

Ji, M., Gao, X.-Y., Zheng, Y.-F. (2022) Geochemical evidence for partial melting of progressively varied crustal sources for leucogranites during the Oligocene–Miocene in the Himalayan orogen. *Chemical Geology* 589, 120674. https://doi.org/10.1016/j.chemgeo.2021.120674

Ji, M., Gao, X.-Y., Zheng, Y.-F. (2023) The petrogenetic relationship between migmatite and granite in the Himalayan orogen: Petrological and geochemical constraints. *Lithos* 444–445, 107110. https://doi.org/10.1016/j.lithos.2023.107110

Kani, T., Misawa, K., Morikawa, N., Kazahaya, K., Kusuhara, F., Yoneda, S., Terakado, Y. (2023) Strontium Isotope Characteristics ($\delta^{88/86}$Sr, ^{87}Sr/^{86}Sr) of Arima-Type Brines Originated From Slab-Fluids. *Geophysical Research Letters* 50, e2022GL100309. https://doi.org/10.1029/2022GL100309

Klaver, M., Lewis, J., Parkinson, I.J., Elburg, M.A., Vroon, P.Z., Kelley, K.A., Elliott, T. (2020) Sr isotopes in arcs revisited: tracking slab dehydration using $\delta^{88/86}$Sr and ^{87}Sr/^{86}Sr systematics of arc lavas. *Geochimica et Cosmochimica Acta* 288, 101–119. https://doi.org/10.1016/j.gca.2020.08.010

Knesel, K.M., Davidson, J.P. (2002) Insights into Collisional Magmatism from Isotopic Fingerprints of Melting Reactions. *Science* 296, 2206–2208. https://doi.org/10.1126/science.1070622

Moynier, F., Agranier, A., Hezel, D.C., Bouvier, A. (2010) Sr stable isotope composition of Earth, the Moon, Mars, Vesta and meteorites. *Earth and Planetary Science Letters* 300, 359–366. https://doi.org/10.1016/j.epsl.2010.10.017

Nesbitt, H.W., Young, G.M. (1982) Early Proterozoic climates and plate motions inferred from major element chemistry of lutites. *Nature* 299, 715–717. https://doi.org/10.1038/299715a0

Ohno, T., Komiya, T., Ueno, Y., Hirata, T., Maruyama, S. (2008) Determination of ^{88}Sr/^{86}Sr mass-dependent isotopic fractionation and radiogenic isotope variation of ^{87}Sr/^{86}Sr in the Neoproterozoic Doushantuo Formation. *Gondwana Research* 14, 126–133. https://doi.org/10.1016/j.gr.2007.10.007

Patiño Douce, A.E., Harris, N. (1998) Experimental Constraints on Himalayan Anatexis. *Journal of Petrology* 39, 689–710. https://doi.org/10.1093/petroj/39.4.689

Powell, R. (1984) Inversion of the assimilation and fractional crystallization (AFC) equations; characterization of contaminants from isotope and trace element relationships in volcanic suites. *Journal of the Geological Society* 141, 447–452. https://doi.org/10.1144/gsjgs.141.3.0447

Sun, S.-s., McDonough, W.F. (1989) Chemical and isotopic systematics of oceanic basalts: implications for mantle composition and processes. *Geological Society, London, Special Publications* 42, 313–345. https://doi.org/10.1144/GSL.SP.1989.042.01.19

Teng, F.-Z., Dauphas, N., Watkins, J.M. (2017) Non-Traditional Stable Isotopes: Retrospective and Prospective. *Reviews in Mineralogy and Geochemistry* 82, 1–26. https://doi.org/10.2138/rmg.2017.82.1

Thomas, R., Davidson, P. (2016) Revisiting complete miscibility between silicate melts and hydrous fluids, and the extreme enrichment of some elements in the supercritical state — Consequences for the formation of pegmatites and ore deposits. *Ore Geology Reviews* 72, 1088–1101. https://doi.org/10.1016/j.oregeorev.2015.10.004

Wu, F.-Y., Liu, X.-C., Liu, Z.-C., Wang, R.-C., Xie, L., Wang, J.-M., Ji, W.-Q., Yang, L., Liu, C., Khanal, G.P., He, S.-X. (2020) Highly fractionated Himalayan leucogranites and associated rare-metal mineralization. *Lithos* 352–353, 105319. https://doi.org/10.1016/j.lithos.2019.105319

Zeng, L., Asimow, P.D., Saleeby, J.B. (2005) Coupling of anatectic reactions and dissolution of accessory phases and the Sr and Nd isotope systematics of anatectic melts from a metasedimentary source. *Geochimica et Cosmochimica Acta* 69, 3671–3682. https://doi.org/10.1016/j.gca.2005.02.035

Zheng, Y.-F., Gao, P. (2021) The production of granitic magmas through crustal anatexis at convergent plate boundaries. *Lithos* 402–403, 106232. https://doi.org/10.1016/j.lithos.2021.106232